

Preparation and electrochemical characterization of $\text{LiNi}_{0.8}\text{Co}_{0.2}\text{O}_2$ cathode material by a modified sol–gel method

Chongqiang Zhu · Chunhui Yang · Wein-Duo Yang ·
Mao-Sung Wu · Huei-Mei Ysai · Ching-Yuan Hsieh ·
Hui-Ling Fang

Received: 29 November 2009 / Accepted: 12 June 2010 / Published online: 10 July 2010
© Springer Science+Business Media B.V. 2010

Abstract $\text{LiNi}_{0.8}\text{Co}_{0.2}\text{O}_2$ cathode powders for lithium-ion batteries were prepared by a modified sol–gel method with citric acid as chelating agent and a small amount of hydroxypropyl cellulose as dispersant agent. The structure and morphology of $\text{LiNi}_{0.8}\text{Co}_{0.2}\text{O}_2$ powders calcined at various temperatures for 4 h in air were characterized by means of powder X-ray diffraction analyzer, scanning electron microscope, thermogravimetric analyzer and differential thermal analyzer, and Brunauer–Emmett–Teller specific surface area analyzer. The results show that $\text{LiNi}_{0.8}\text{Co}_{0.2}\text{O}_2$ powders calcined at 800 °C exhibit the best layered structure ordering and appear to have monodispersed particulates surface. In addition, the electrochemical properties of $\text{LiNi}_{0.8}\text{Co}_{0.2}\text{O}_2$ powders as cathode material were investigated by the charge–discharge and cyclic voltammetry studies in a three-electrode test cell. The initial charge–discharge studies indicate that $\text{LiNi}_{0.8}\text{Co}_{0.2}\text{O}_2$ cathode material obtained from the powders calcined at 800 °C shows the largest charge capacity of 231 mAh g⁻¹ and the largest discharge capacity of 191 mAh g⁻¹. And, the cyclic voltammetry studies

indicate that Li^+ insertion and extraction in $\text{LiNi}_{0.8}\text{Co}_{0.2}\text{O}_2$ powders is reversible except for the first cycle.

Keywords $\text{LiNi}_{0.8}\text{Co}_{0.2}\text{O}_2$ · Sol–gel method · Calcination temperature · Cyclic voltammetry · Charge–discharge

1 Introduction

The layered LiCoO_2 is currently the most prevailing cathode material for the commercial lithium-ion batteries [1]. However, the high cost and inherent toxicity of the material limit its widespread progress in lithium-ion batteries [2–4]. Recently, LiNiO_2 is considered as an attractive cathode material due to its higher discharge capacity and lower cost [5]. But, LiNiO_2 also has several disadvantages, such as difficult stoichiometry control in the preparation process, poor cycling performance, and unsatisfactory thermal stability [5–7]. Hence, to improve the electrochemical properties of LiNiO_2 , a great deal of research has been attempted by doping the material with several transition metals [8–11], of which cobalt doping revealed excellent performance.

The doped $\text{LiNi}_{1-x}\text{Co}_x\text{O}_2$ ($0 < x < 1$) compounds are solid solutions having the same layered $\alpha\text{-NaFeO}_2$ structure as LiCoO_2 and LiNiO_2 [12]. $\text{LiNi}_{1-x}\text{Co}_x\text{O}_2$ compounds have the merits of both LiCoO_2 and LiNiO_2 [13–15], such as lower cost, higher capacity and less toxicity than LiCoO_2 , easy to prepare, better cyclability and higher thermal stability than LiNiO_2 . Among these compounds, $\text{LiNi}_{0.8}\text{Co}_{0.2}\text{O}_2$ has been identified as one of the most promising materials to replace LiCoO_2 and as a potential next generation cathode material for lithium-ion batteries [16–18].

C. Zhu · C. Yang
Department of Applied Chemistry, Harbin Institute
of Technology, Harbin 150001, People's Republic of China

W.-D. Yang (✉) · M.-S. Wu · H.-L. Fang
Department of Chemical and Materials Engineering,
National Kaohsiung University of Applied Sciences,
Kaohsiung 807, Taiwan
e-mail: ywd@cc.kuas.edu.tw

H.-M. Ysai · C.-Y. Hsieh
Materials and Electro-Optics Research Division Battery Section,
Chung-Shan Institute of Science and Technology, Lung-Tan,
Tao-Yuan 325, Taiwan

Traditionally, $\text{LiNi}_{1-x}\text{Co}_x\text{O}_2$ compounds are prepared by solid-state reaction at high temperatures for a long time period [19]. However, the method has several drawbacks [20, 21], such as irregular morphology, poor stoichiometry control, inhomogeneity, and large particle size, which could affect the electrochemical properties of $\text{LiNi}_{1-x}\text{Co}_x\text{O}_2$. Several solution methods have been proposed to improve the structure and morphology of $\text{LiNi}_{1-x}\text{Co}_x\text{O}_2$, of which the sol–gel method is an optimal alternative technology to overcome these problems [22, 23]. The sol–gel method has been used to prepare $\text{LiNi}_{1-x}\text{Co}_x\text{O}_2$ at lower temperature and shorter time, and mostly, compound powders with uniform morphology, narrow particle size distribution, and high homogeneity can be obtained.

In this study, $\text{LiNi}_{0.8}\text{Co}_{0.2}\text{O}_2$ powders were obtained after calcining the precursors prepared by the sol–gel method with citric acid as the chelating agent. The effect of calcination temperature, which is the essential influencing factor in the sol–gel preparation process, on the structure and morphology of $\text{LiNi}_{0.8}\text{Co}_{0.2}\text{O}_2$ powders was examined by several detection technologies. Furthermore, the relationship between the calcination temperature and the cycling performances and charge/discharge characteristics of $\text{LiNi}_{0.8}\text{Co}_{0.2}\text{O}_2$ was investigated in detail.

2 Experimental

2.1 Preparation of $\text{LiNi}_{0.8}\text{Co}_{0.2}\text{O}_2$ powders

$\text{LiNi}_{0.8}\text{Co}_{0.2}\text{O}_2$ powders were prepared by the sol–gel method using LiNO_3 (SHOWA, 99.5%), $\text{Ni}(\text{NO}_3)_2 \cdot 6\text{H}_2\text{O}$ (SHOWA, 98%), and $\text{Co}(\text{NO}_3)_2 \cdot 6\text{H}_2\text{O}$ (Baker, 99.8%) as starting materials, de-ionized water as solvent, citric acid ($\text{C}_6\text{H}_8\text{O}_7 \cdot \text{H}_2\text{O}$, Riedel-de Haen, 99.5%) as chelating agent, and hydroxypropyl cellulose (ALDRICH, M = 10^5) as dispersant agent. The stoichiometric amounts of lithium, nickel, and cobalt nitrate salts (Li:Ni:Co = 1:0.8:0.2 M ratio) were dissolved separately in de-ionized water. Then, a solution containing certain amount of citrate (the molar ratio of citric acid/total metal ions = 1) and mixed completely with a small amount of hydroxypropyl cellulose (the molar ratio of cellulose-to-total cations was 5×10^{-6}) was obtained using a suitable amount of de-ionized water as solvent. The individual solutions were mixed, and then the mixed solution was heated at 65 °C for 3 h under constant stirring to form the sol. The sol was then evaporated at 120 °C in dry oven until the gel was formed. $\text{LiNi}_{0.8}\text{Co}_{0.2}\text{O}_2$ powders were obtained by calcining gel precursors in air at various temperatures between 300 and 900 °C for 4 h. The preparation procedure of $\text{LiNi}_{0.8}\text{Co}_{0.2}\text{O}_2$ powders by a modified sol–gel method is shown in Fig. 1.

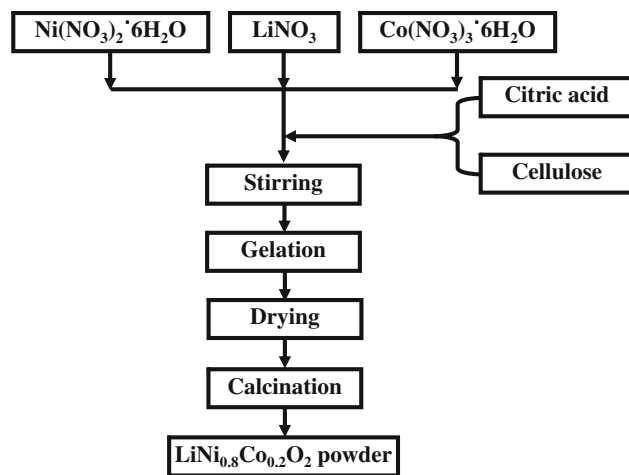


Fig. 1 The preparation procedure of $\text{LiNi}_{0.8}\text{Co}_{0.2}\text{O}_2$ powders by a modified sol–gel method

2.2 Characterization

The thermal decomposition behavior of gel precursors was examined by means of thermogravimetric analyzer and differential thermal analyzer (TGA/DTA, Du Pont, SDT2960) at a heating rate of 10 °C min⁻¹ up to 1000 °C in air. The crystalline phase of $\text{LiNi}_{0.8}\text{Co}_{0.2}\text{O}_2$ powders was identified by means of powder X-ray diffraction analyzer (XRD, Rigaku, Rint-2000) with Cu K α at a scanning rate of 4° min⁻¹ between 15° and 80°. The surface morphology of $\text{LiNi}_{0.8}\text{Co}_{0.2}\text{O}_2$ powders was observed by means of scanning electron microscope (SEM, JEOL, S-5610). The specific surface area of $\text{LiNi}_{0.8}\text{Co}_{0.2}\text{O}_2$ powders was determined by means of Brunauer–Emmett–Teller analyzer (BET, Micromeritics, ASAP2101) with low-temperature argon absorption. Moreover, the as-prepared $\text{LiNi}_{0.8}\text{Co}_{0.2}\text{O}_2$ powders were also dissolved in the 2 M HCl solution. The contents of Li, Ni, and Co were characterized by atomic absorption spectroscopy (AA).

2.3 Electrochemical properties measurement

The electrochemical properties of $\text{LiNi}_{0.8}\text{Co}_{0.2}\text{O}_2$ were measured with three-electrode cells. The cathode was prepared by mixing 85 wt% $\text{LiNi}_{0.8}\text{Co}_{0.2}\text{O}_2$ powders, 10 wt% carbon black, and 5 wt% PTFE in ethanol solvent. The resulting slurry was pressed on an oblong nickel foil (20 × 10 mm) which was then dried at 250 °C in an oven. The counter electrode and the reference electrode were Pt wire and saturated calomel electrode (SCE), respectively. The electrolyte was 1 M Li_2SO_4 , of which the solution pH was corrected to 8–10 by LiOH addition. Cyclic voltammetry was performed on a CHI 611C electrochemical workstation at room temperature with a scan rate of 1 mV s⁻¹ between 0 and 1.2 V (vs. SCE). The charge/

discharge measurement was performed on a LAND CT2001A testing system with a 0.5 C rate between 0 and 1.2 V (vs. SCE).

Further, 1 M LiPF₆ (electrolyte) containing a solution of ethylene carbonate (EC) and diethylene carbonate (DEC) (1:1 in weight) was also utilized as a non-aqueous electrolyte (LiPF₆ + EC + DEC), again. The electrochemical cells were then assembled in an Ar filled glovebox using foils of Li metal as counter electrodes. However, the electrochemical measurements were performed in the voltage range 3.0–4.2 V using a galvanostatic charge/discharge cycler at a current rate of 0.5 C for 30 cycles.

3 Results and discussion

The gel precursors were the intermediate products before transforming to LiNi_{0.8}Co_{0.2}O₂ powders. The thermal behavior of the gel precursors affects the process condition, the particle size and the specific surface area of the powders, and the lattice parameter. The TGA–DTA curves of the gel precursors are shown in Fig. 2. Three discrete weight loss steps are observed in the TGA curve. The initial weight loss step at below 200 °C is associated with the removal of the residual water. The secondary weight loss region occurred at 200–380 °C, which corresponds to a large peak of the exothermic reaction around 360 °C in the DTA curve, is due to the decomposition of citric acid and nitrates. The last weight loss region occurred at 380–600 °C, which corresponds to two small peaks of the exothermic reactions around 480 and 520 °C in the DTA curve, is due to the combustion of the residual organic constituents. Since there is no weight loss over 600 °C, the formation temperature of LiNi_{0.8}Co_{0.2}O₂ powders is as low as 600 °C.

The structure and morphology of LiNi_{0.8}Co_{0.2}O₂ powders are dependent on the calcination temperature. The optimum calcination temperature for the preparation process is determined by the following techniques.

The XRD patterns of LiNi_{0.8}Co_{0.2}O₂ powders calcined at various temperatures for 4 h in air are shown in Fig. 3. When LiNi_{0.8}Co_{0.2}O₂ powders were calcined at 300 °C, no signal is observed from the powders which implies that the powders calcined at the temperature is still amorphous and there is no formation of any crystalline phase. For LiNi_{0.8}Co_{0.2}O₂ powders were calcined at 400 and 500 °C, none of the peaks characteristic to powders is observed and only impurity peaks are present which are attributed to LiNO₃, Li₂CO₃, and NiO phase. It is obviously found that the calcination temperature increases, the characteristic peaks of LiNi_{0.8}Co_{0.2}O₂ phase become sharper and stronger, suggesting that the crystallinity of LiNi_{0.8}Co_{0.2}O₂ powders is improved as increasing the calcination

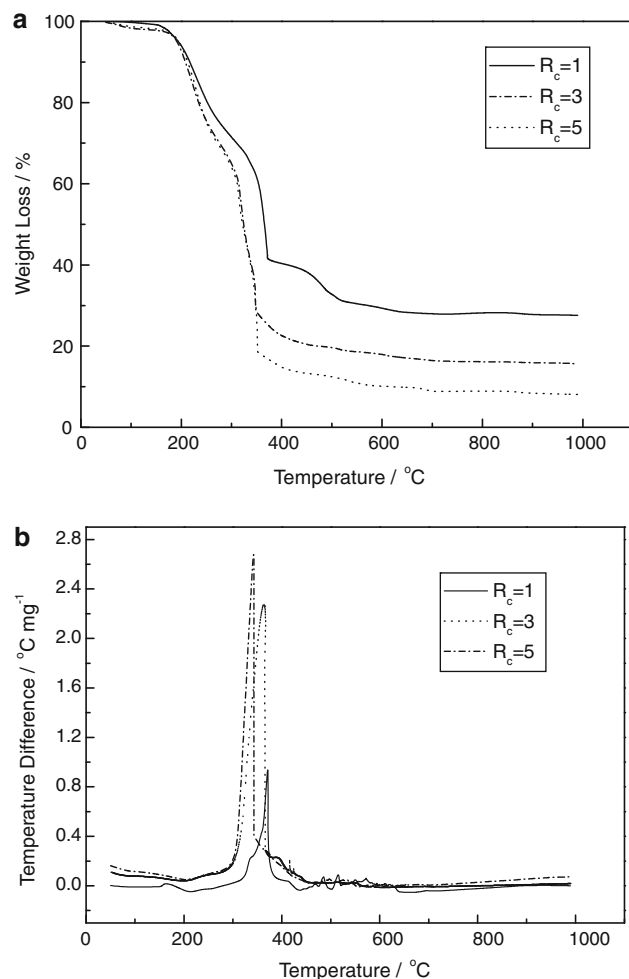


Fig. 2 TGA–DTA curves of the gel precursors. **a** TGA curves of the dried gels prepared from various molar ratios of citric acid/metal ions (R_c). **b** DTA curves of the dried gels prepared from various molar ratios of citric acid/metal ions (R_c)

temperature. In particular, LiNi_{0.8}Co_{0.2}O₂ powders calcined at 800 °C shows a clearer splitting of the (006)/(102) peaks and a better symmetry of the (108)/(110) peaks than the powders calcined at other temperatures, namely LiNi_{0.8}Co_{0.2}O₂ powders calcined at 800 °C has more layered structure. Besides the degree of splitting the peaks (006)/(102) and (108)/(110), the unit cell volume is also as a criterion to judge the ordering of a layered structure [24]. The lower the unit cell volume, the more will be the layered structure. For LiNi_{0.8}Co_{0.2}O₂ powders calcined at 800 °C, the unit cell volume is 101 Å³, while for the powders calcined at 600, 700, and 900 °C, the respective volume are 102, 101, and 103 Å³, respectively. The unit cell volume is decreased with increasing the calcination temperature from 600 to 800 °C, which is due to the complete ordering of cations in the powders at higher temperature. But for 900 °C, the unit cell volume is increased.

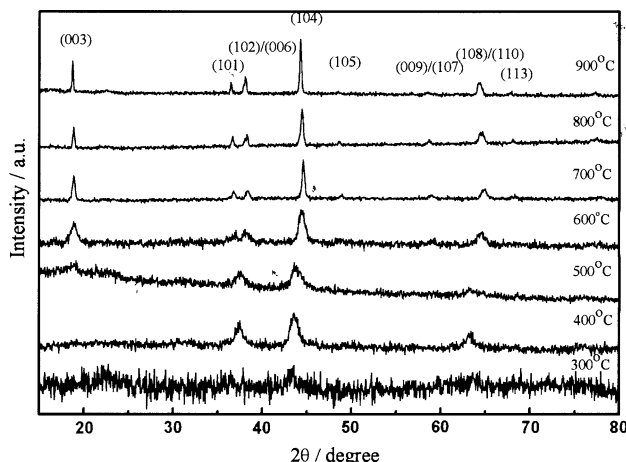


Fig. 3 X-ray diffraction patterns of $\text{LiNi}_{0.8}\text{Co}_{0.2}\text{O}_2$ powders calcined at various temperatures

Table 1 Crystal properties and chemical analysis of the $\text{LiNi}_{0.8}\text{Co}_{0.2}\text{O}_2$ powders calcined at various temperatures for 4 h in air

Temperature (°C)	Unit cell volume (\AA^3)	R-factor $[(I_{(006)} + I_{(102)})/I_{(101)}]$	Molar ratio		
			Li	Ni	Co
600	102	a	1.03	0.80	0.202
700	101	1.95	1.02	0.80	0.202
800	101	1.83	0.99	0.80	0.198
900	103	2.14	0.96	0.80	0.196

^a 006/102 splitting is not discernable to determine R

Lithium, nickel, and cobalt molar ratios of the $\text{LiNi}_{0.8}\text{Co}_{0.2}\text{O}_2$ powders calcined at various temperatures were measured by AA as listed in Table 1. It indicates that the molar ratios of lithium, nickel, and cobalt were very close to the original design of starting materials at 1.00:0.80:0.20. As calcined at 900 °C, a relatively small amount of lithium was examined, because the evaporation of lithium during calcination at high temperature. It results the molar ratio of $\text{Li}/(\text{Ni} + \text{Co})$ deviated from the stoichiometric ratio of 1.0 in the calcined powders. Since a small amount of Li volatilized at the temperature results in Ni^{3+} moving into the Li sites, the layered structure of the $\text{LiNi}_{0.8}\text{Co}_{0.2}\text{O}_2$ powders is slightly distorted.

The R-factor is defined as the ratio of the intensities of the double peaks (006) and (102) to the (101) peak, and indicates the characteristic of hexagonal ordering. The lower the R-factor, the better is the hexagonal ordering. The R-factor of $\text{LiNi}_{0.8}\text{Co}_{0.2}\text{O}_2$ powders calcined at various temperatures is listed in Table 1. The $\text{LiNi}_{0.8}\text{Co}_{0.2}\text{O}_2$ powder calcined at 600 °C exhibiting the (006) and (102) splitting is not discernable, revealing a lower layered structure ordering. Nevertheless, the powder obtained at 800 °C, R-factor is 1.83, it possesses a good hexagonal

ordering. But, the R-factor of the powder is 2.14 as calcined at 900 °C, as well as the (006) and (102) peaks also become hardly distinguishable, demonstrating the decreasing of hexagonal ordering as comparing with the powder prepared at 800 °C.

As seen from Table 1, a relatively small amount of lithium was examined as the powder calcined at 900 °C, indicates the evaporation of lithium ion during the high calcination temperature. Moreover, a large R-factor was also found to reveal the lower cations mixing ordering at the high calcination temperature.

In the case, the nickel-substituted phases, $\text{LiNi}_{0.8}\text{Co}_{0.2}\text{O}_2$, it is known that the existence of nickel ions in the lithium layers, because of the propensity of nickel ion to mix with the lithium layer as often obtains in LiNiO_2 . However, the presence of Ni^{3+} in the Li^+ sites is also believed to impede diffusion of lithium ions in the host lattice. Thus, it can be predicted that the loss of the electrode ability of full Li de-intercalation corresponding to an appearance of structural defects in $\text{LiNi}_{0.8}\text{Co}_{0.2}\text{O}_2$ electrode as calcined at 900 °C.

Based on the above results, it can be concluded that the optimum calcination temperature required for complete layered $\text{LiNi}_{0.8}\text{Co}_{0.2}\text{O}_2$ powders is 800 °C. The SEM micrographs of $\text{LiNi}_{0.8}\text{Co}_{0.2}\text{O}_2$ powders calcined at various temperatures for 4 h in air are presented in Fig. 4. As shown in this figure, the particle size of $\text{LiNi}_{0.8}\text{Co}_{0.2}\text{O}_2$ powders is increased with increasing the calcination temperature, which indicates that the crystal growth is accelerated at higher temperature leading to the agglomeration of spherical particles to larger particulates. Moreover, the powders calcined at different temperatures are comprised of particles with similar shape and size. $\text{LiNi}_{0.8}\text{Co}_{0.2}\text{O}_2$ powders calcined at 800 °C, the optimum calcination temperature, appears to a particulate shape of average size 1500–2000 Å. The specific surface area of $\text{LiNi}_{0.8}\text{Co}_{0.2}\text{O}_2$ powders calcined at 600, 650, and 700 °C is 15.58, 10.73, and $4.08 \text{ m}^2 \text{ g}^{-1}$, respectively, indicating that the specific surface area of the powders is increased as the calcination temperature is increased. The conclusion is consistent with the SEM observation.

The electrochemical performances of $\text{LiNi}_{0.8}\text{Co}_{0.2}\text{O}_2$ powders calcined at various temperatures for 4 h were examined between 0 and 1.2 V. Figure 5 shows the initial charge–discharge profiles of $\text{LiNi}_{0.8}\text{Co}_{0.2}\text{O}_2$ powders calcined at various temperatures at a rate of 0.1 C. The charge capacities of $\text{LiNi}_{0.8}\text{Co}_{0.2}\text{O}_2$ powders calcined at 600, 700, and 800 °C are 151, 204, and 231 mAh g⁻¹, respectively, and the discharge capacities of the powders calcined at the same temperatures are 125, 176, and 191 mAh g⁻¹, respectively. Therefore, the charge–discharge capacity is significantly increased upon increasing the calcination temperature, of which $\text{LiNi}_{0.8}\text{Co}_{0.2}\text{O}_2$ powders calcined at

Fig. 4 Scanning electron micrographs of $\text{LiNi}_{0.8}\text{Co}_{0.2}\text{O}_2$ powders calcined at various temperatures. **a** 600 °C, **b** 700 °C, **c** 800 °C, and **d** 900 °C

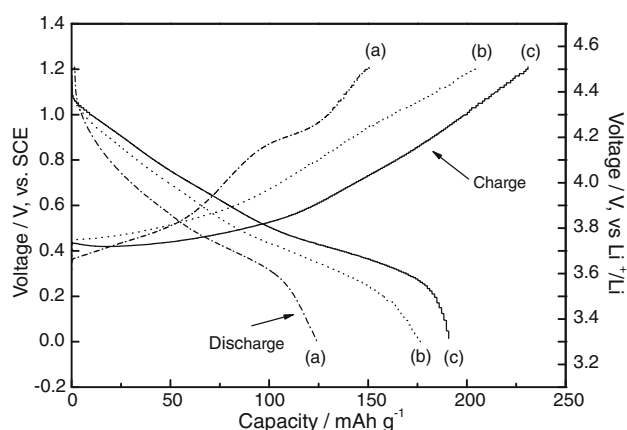
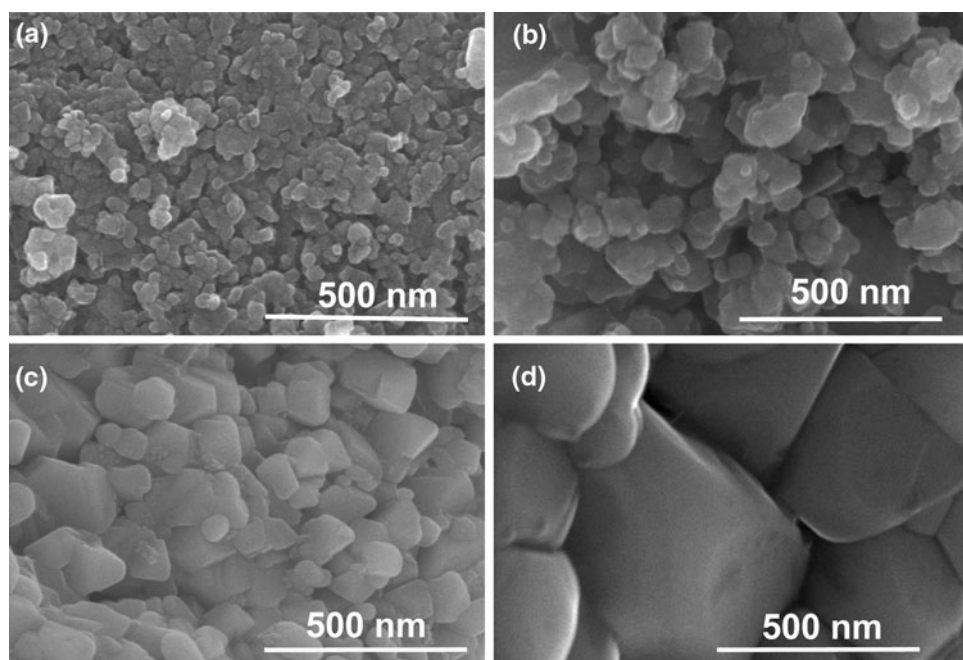


Fig. 5 Initial charge–discharge profiles of $\text{LiNi}_{0.8}\text{Co}_{0.2}\text{O}_2$ powders calcined at various temperatures: (a) 600 °C, (b) 700 °C, and (c) 800 °C

800 °C have the highest charge–discharge capacity. It means that $\text{LiNi}_{0.8}\text{Co}_{0.2}\text{O}_2$ powders calcined at 800 °C have the complete layered structure, in other words, i.e. the optimum calcination temperature for the preparation $\text{LiNi}_{0.8}\text{Co}_{0.2}\text{O}_2$ powders preparation is 800 °C. The conclusions also strongly confirm the results obtained from XRD measurement.

Figure 6 shows the cyclic voltammetry (CV) results of $\text{LiNi}_{0.8}\text{Co}_{0.2}\text{O}_2$ powders calcined at 800 °C at a scan rate of 1 mV s⁻¹. In general, the anodic and cathodic peaks observed in the cyclic voltammograms of $\text{LiNi}_{0.8}\text{Co}_{0.2}\text{O}_2$ cathode material reflect reversible oxidation and reduction reactions corresponding to Li^+ extraction and insertion. The behavior of the first cycle is different from that of the

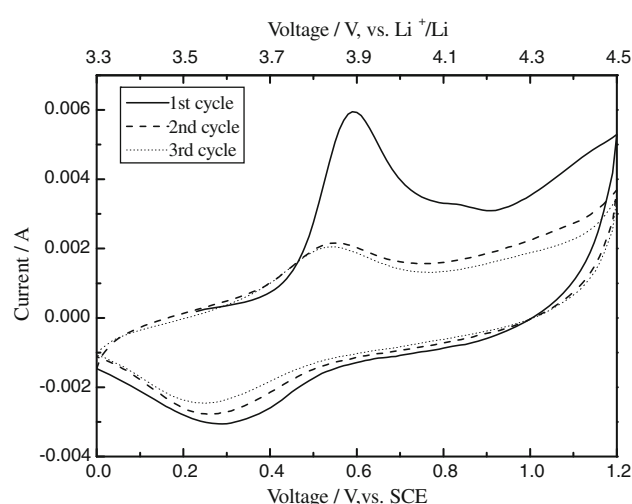


Fig. 6 Cyclic voltammograms of $\text{LiNi}_{0.8}\text{Co}_{0.2}\text{O}_2$ powders calcined at 800 °C

subsequent two cycles. At the first cycle, the oxidation peak is observed at 0.60 V, while the oxidation peak of the second cycle is located at 0.55 V. Furthermore, the corresponding peak current at the first peak is three times as big as that of the second peak. These observations indicate that a large irreversible capacity occurs in the first cycle, which is owing to the irreversible oxidation of the extra Ni^{2+} in the $\text{LiNi}_{0.8}\text{Co}_{0.2}\text{O}_2$ cathode material at the first cycle resulting in a local shrinking of the layered structure, and hence restricting Li^+ reintercalation. The shapes of the second and the third cycles are similar, which indicates the quantitative reversibility of Li^+ extraction and insertion in the $\text{LiNi}_{0.8}\text{Co}_{0.2}\text{O}_2$ cathode material.

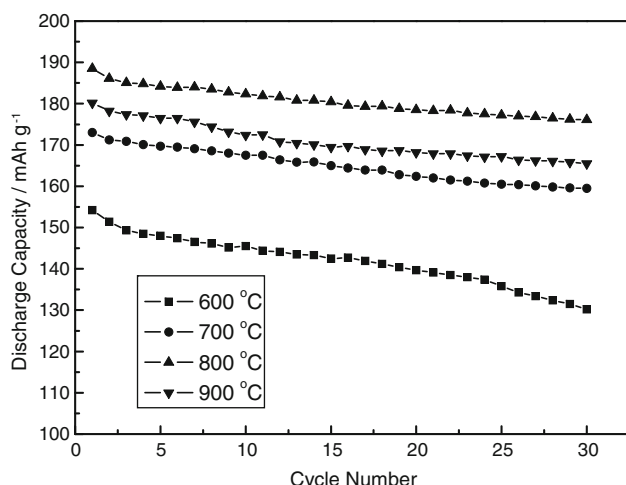


Fig. 7 The discharge capacity of $\text{LiNi}_{0.8}\text{Co}_{0.2}\text{O}_2$ electrodes in a non-aqueous electrolyte ($\text{LiPF}_6 + \text{EC} + \text{DEC}$) examined in the voltage range 3.0–4.2 V and a current rate of 0.5 C for 30 cycles

Figure 7 shows the discharge capacity of $\text{LiNi}_{0.8}\text{Co}_{0.2}\text{O}_2$ electrodes in a non-aqueous electrolyte ($\text{LiPF}_6 + \text{EC} + \text{DEC}$) examined in the voltage range 3.0–4.2 V and a current rate of 0.5 C for 30 cycles. It indicates that the capacities of the first several cycles were relatively high, but were improved remarkably after the several cycles. After 30 cycles, the discharge capacity for 600, 700, 800, and 900 °C is 130.2, 159.5, 176.1, and 165.5 mAh g^{-1} , respectively.

The prediction based on the results of XRD studies of the prepared $\text{LiNi}_{0.8}\text{Co}_{0.2}\text{O}_2$ powders, the powders prepared at 600 °C exhibits low discharge capacity of 154.2 mAh g^{-1} (first cycle). The discharge capacity of the $\text{LiNi}_{0.8}\text{Co}_{0.2}\text{O}_2$ cathode increases as the temperature of calcination is increased from 600 to 800 °C. Nevertheless, the discharge capacity is decreased for the powder calcined at 900 °C. It may be attributed to the appearance of structural defects of cations mixing disorder that makes the intercalation/de-intercalation difficult.

4 Conclusions

$\text{LiNi}_{0.8}\text{Co}_{0.2}\text{O}_2$ powders were prepared by the sol-gel method using citric acid as chelating agent at various calcination temperatures for 4 h in air. The optimum calcination temperature for $\text{LiNi}_{0.8}\text{Co}_{0.2}\text{O}_2$ powders with complete ordering layered structure is 800 °C, which is due to the most obvious separations of the (006)/(102) peaks and the (008)/(110) peaks, and the lowest volume of the unit cell. Moreover, the surface of $\text{LiNi}_{0.8}\text{Co}_{0.2}\text{O}_2$ powders calcined at 800 °C displays monodispersed particulates

with an average particle size of 1500–2000 Å. In the three-electrode test cells, the initial charge-discharge experiments indicate that $\text{LiNi}_{0.8}\text{Co}_{0.2}\text{O}_2$ powders calcined at 800 °C as the cathode material exhibit the largest charge capacity, at 231 mAh g^{-1} , and the largest discharge capacity, at 191 mAh g^{-1} . However, the best layered structure of $\text{LiNi}_{0.8}\text{Co}_{0.2}\text{O}_2$ phase was obtained as the powders calcined at 800 °C. In addition, the cyclic voltammetric studies suggest that the irreversible capacity arises only in the first cycle due to the irreversible oxidation of the extra Ni^{2+} while with further cycling, Li^+ insertion and extraction in $\text{LiNi}_{0.8}\text{Co}_{0.2}\text{O}_2$ powders maintains good reversibility.

Acknowledgments The authors gratefully acknowledge the financial support of the National Science Council of the Republic of China (Taiwan).

References

- Predoana L, Barau A, Zaharescu M, Vassilchina H, Velinova N, Banov B, Momchilov A (2007) J Eur Ceram Soc 27:1137
- Oh SH, Jeong WT, Cho WI, Cho BW, Woo K (2005) J Power Sources 140:145
- Julien C, Michael SS, Ziolkiewicz S (1999) Int J Inorg Mater 1:29
- Wang M, Navrotsky A (2004) Solid State Ionics 166:167
- Sun Y, Wan P, Pan J, Xu C, Liu X (2006) Solid State Ionics 177:1173
- Yamada S, Fujiwara M, Kanda M (1995) J Power Sources 54:209
- Periasamy P, Kim HS, Na SH, Moon SI, Lee JC (2004) J Power Sources 132:213
- Periasamy P, Kalaiselvi N (2006) J Power Sources 159:1360
- Guo X, Greenbaum S, Ronci F, Scrosati B (2004) Solid State Ionics 168:37
- Kim J, Amine K (2002) J Power Sources 104:33
- Saadoune I, Delmas C (1998) J Solid State Chem 136:8
- Babu BR, Periasamy P, Thirunakaran R, Kalaiselvi N, Prem Kumar T, Renganathan NG, Raghavan M, Muniyandi N (2001) Int J Inorg Mater 3:401
- Fey GTK, Yo WH, Chang YC (2002) J Power Sources 105:82
- Gross T, Buhrmester T, Bramnik KG, Bramnik NN, Nikolowski K, Baehtz C, Ehrenberg H, Fuess H (2005) Solid State Ionics 176:1193
- Delmas C, Saadoune I (1992) Solid State Ionics 53–56:370
- Gover R, Kanno R, Mitchell B, Hirano A, Kawamoto Y (2000) J Power Sources 90:82
- Lu W, Lee CW, Venkatachalapathy R, Prakash J (2000) J Appl Electrochem 30:1119
- Yang Z, Wang B, Yang W, Wei X (2007) Electrochim Acta 52:8069
- Cho TH, Chung HT (2005) J Appl Electrochem 35:1033
- Fey GTK, Subramanian V, Lu CZ (2002) Solid State Ionics 152–153:83
- Ying J, Wan C, Jiang C, Li Y (2001) J Power Sources 99:78–84
- Fey GTK, Subramanian V, Chen JG (2002) Mater Lett 52:197
- Fey GTK, Chen JG, Wang ZF, Yang HZ, Kumar TP (2004) Mater Chem Phys 87:246
- Dahn JR, Sacken UV, Michal CA (1990) Solid State Ionics 44:87